Numerical Simulation of Stress Change during Wellbore Injection

Mahmood Bataee[1,a] and Sonny Irawan[1,b]

[1]Petroleum Engineering Department, Universiti Teknologi PETRONAS (UTP), Seri Iskandar, Perak, Malaysia

[a]mahmood_bataee@hotmail.com, [b]drsonny_irawan@petronas.com.my

Keywords: Failure criteria, Wellbore studies, Stress State, Stability, Review

Abstract. The important matter during any process in the well is wellbore integrity. Regarding to the geomechanics of the well, high bottom-hole pressure and low temperature could lead to the fracturing. The stress near the wellbore is a function of the flow and temperature, and it precisely determined to avoid the wellbore failure. The objective of this paper is to simulate stress change in the well for the injection. The stress calculated for different pressures, temperature, and in-situ stresses states.

In order to analyze the stress in the wellbore a finite volume analysis has done for the wellbore. The stress equation relates to flow equation with the equation of principle stress. It means that the pressure is a key parameter for determination of the stress. The procedure which has to be followed is transforming the equations to weak form, meshing the defined shape and programing to obtain the values for each node. The result for the stress is obtained for some meshed bodies. The accuracy enhanced by choosing smaller mesh sizing.

Introduction

Rocks are combination of different materials. But, the rocks have poro-elastic response. The amount of the stress indexed by the pore pressure depends on its pore content. The study of the stress in two phase medium and void space is essential for the well integrity in oil production from the well. The study of the temperature is also important in defining the stress. The theory of thermo-poroelasticity (or porothermoelasticity) is developed by combining the influence of thermal stress and the difference between solid and fluid expansion.

An early attempt of applying the stress to the reservoir state had done by Espinoza (1983). Some formula that relates the pressure and temperature to the pore compressibility had used in the study to obtain the compaction in the steam injection model. He changes the rock properties and reach to some results; as the change in permeability resulted from pore volume alteration is not considerable. The results were primeval but it was an ignition for further studies.

In 1987 Lewis and Schrefler had published the first edition of the book of deformation in porous media. They had collected the formula of flow and stress and provide mathematical models to solve the equations. They had modified their work some years later.

Settari et al. (1999) expressed the idea of reservoir flow analysis coupling with reservoir geomechanics. As they had explained, reservoir simulators ignore the geomechanical aspect of porous rocks. They had considered the effect of pressure and temperature on stress and had applied it in a field study. They had also studied different coupling and compaction models. They used the experimental studies to calibrate the rock characteristics and input the parameter into the simulator. Their attempts were the basis of the many works afterwards. Although their results were interesting, the study suffers of obsolete formula and boundary conditions.

Chin et al. (2002) had used an iterative procedure for coupled analysis of multi-phase flow and geomechanics in reservoir simulator. They had examined the rocks with other compaction behaviors. They had presented the descriptions of formulations, solution procedures, and strategies for enhancement of computational efficiency in their paper. Also some different boundary conditions had been applied as large-scale field examples.

Mendes et al. (2012) had done a study of coupling with heterogeneity. They get their special boundary conditions and solve the two-phase flow problem using Monte Carlo algorithm. They

reach to the result of locally conservative numerical solution and impress that there is an obvious change in production resulted by heterogeneity.

METHODOLOGY

The FVM method have been used to determine the stress. The stress equation is the main equation which should be discretized. The change in pressure and temperature are ignored in this part, and only a distribution of pressure and temperature had used.

The flow chart of the study in this part is expressed in Figure 1. In order to find the stress and strain these procedure has to be followed. First the equation should transport into weak form, and be ready to be solved for each node. Then the body shape of the study has to be meshed. The program had been developed to find the strain and subsequently stress for any tetrahedral meshed body. The feed of the program is the initial and boundary conditions, position of the nodes and the connectivity of them. In this paper two different shapes have been studied. First, the simple cube and then the wellbore shape body.

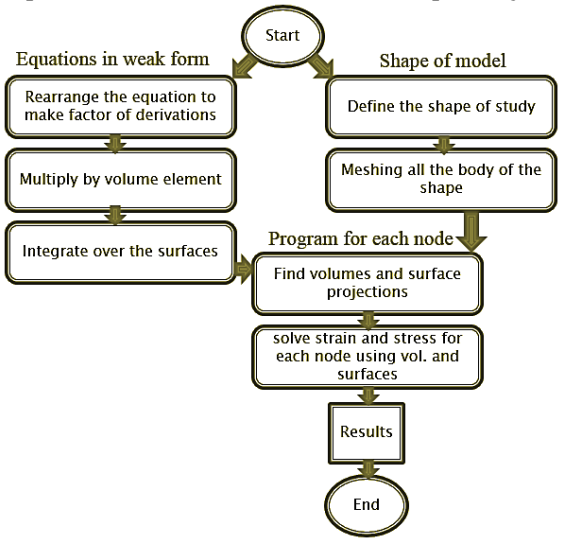

Figure 1: The stress and strain calculated using FVM.

Weak Form of Equations

The equations should transform to the weak form, in order to feed into the FVM. As it mentioned before, in this part of study the pressure and temperature distribution remains constant. The main equation in this part is stress equation (1), which f is the body force and assumed zero in this case.

$$div\ \sigma - f = 0 \quad (1)$$

The equation of the poro-elasticity defines the relation between stress and strain.

$$\sigma_{ij} = \lambda\varepsilon_{vol}\delta_{ij} + 2G\varepsilon_{ij} + 3\alpha_T K(T - T_0)\delta_{ij} - C\zeta \quad (2)$$

Which ζ is the strain of the shear part and could be written in this form:

$$\zeta = \phi\left(\frac{1}{K_s} - \frac{1}{K_f}\right)\bar{p}_f \quad (3)$$

The volumetric strain ε_{vol} is the following equation:

$$\varepsilon_{vol} = \varepsilon_x + \varepsilon_y + \varepsilon_z \quad (4)$$

Which strain in x, y and z direction are as followed (5-7).

$$\varepsilon_x = \frac{\delta u}{\delta x} \quad (5)$$

$$\varepsilon_y = \frac{\delta v}{\delta y} \quad (6)$$

$$\varepsilon_z = \frac{\delta w}{\delta z} \quad (7)$$

Hence, the equation (31) becomes in the form of equations (8-10).

$$\lambda\left(\frac{\delta^2 u}{\delta x^2} + \frac{\delta^2 v}{\delta y^2} + \frac{\delta^2 w}{\delta z^2}\right) + 2G\frac{\delta^2 u}{\delta x^2} + 3\alpha_T K\frac{\delta T}{\delta x} - C\,\phi\left(\frac{1}{K_s} - \frac{1}{K_f}\right)\frac{\delta\bar{p}_f}{\delta x} = 0 \quad (8)$$

$$\lambda\left(\frac{\delta^2 u}{\delta x^2} + \frac{\delta^2 v}{\delta y^2} + \frac{\delta^2 w}{\delta z^2}\right) + 2G\frac{\delta^2 v}{\delta y^2} = constant \quad (9)$$

$$\lambda\left(\frac{\delta^2 u}{\delta x^2} + \frac{\delta^2 v}{\delta y^2} + \frac{\delta^2 w}{\delta z^2}\right) + 2G\frac{\delta^2 w}{\delta z^2} = constant \quad (10)$$

Which the matrix becomes in the format of equation (11), in which u, v and w are the deformation in the x, y and z directions.

$$\begin{bmatrix} & \cdots & \\ \vdots & \ddots & \vdots \\ & \cdots & \end{bmatrix}_{*3} \begin{bmatrix} u \\ v \\ w \end{bmatrix}_{3*1} = \begin{bmatrix} 0 \\ 0 \\ 0 \end{bmatrix}_{3*1} \quad (11)$$

Here, the procedure to change the equation to the weak form begins, and the equations for one direction (x-direction) is written here. For the others, the procedure is the same. The factor is taken from the equations and the derivation of u over x transforms to F ($F = \frac{\delta u}{\delta x}$). The same procedure is to obtain G and H. The G in the equation (12) is module of rigidity (shear modulus) and it is different from G in the equation (13), which is the strain in y-direction.

$$\lambda\left(\frac{\delta^2 u}{\delta x^2} + \frac{\delta^2 v}{\delta y^2} + \frac{\delta^2 w}{\delta z^2}\right) + 2G\frac{\delta}{\delta x}\left(\frac{\delta u}{\delta x}\right) = constant \quad (12)$$

After the transformation, the marix becomes in the format of equation (42).

$$\begin{bmatrix} & \cdots & \\ \vdots & \ddots & \vdots \\ & \cdots & \end{bmatrix}_{*3} \begin{bmatrix} F \\ G \\ H \end{bmatrix}_{3*1} = \begin{bmatrix} 0 \\ 0 \\ 0 \end{bmatrix}_{3*1} \quad (13)$$

Therefore, this new equation is obtained.

$$\lambda\left(\frac{\delta F}{\delta x} + \frac{\delta G}{\delta x} + \frac{\delta H}{\delta x}\right) + 2G\frac{\delta F}{\delta x} = constant \quad (14)$$

The equations should be multiplied by the unit volume.

$$\lambda(F\Delta z\Delta y + \bar{G}\Delta z\Delta y + \bar{H}\Delta z\Delta y) + 2GF\Delta z\Delta y = constant * v_i \quad (15)$$

After rearranging these equation obtain (16-18). Therefore, they should be solved for every single node.

$$\frac{1}{\Omega_i}\lambda(F\Delta sx + \bar{G}\Delta sx + \bar{H}\Delta sx) + 2GF\Delta sx = constant \quad (16)$$

$$\frac{1}{\Omega_i}\lambda(\bar{F}\Delta sy + G\Delta sy + \bar{H}\Delta sy) + 2GG\Delta sy = constant \quad (17)$$

$$\frac{1}{\Omega_i}\lambda(\bar{F}\Delta sz + \bar{G}\Delta sz + H\Delta sz) + 2GH\Delta sz = constant \quad (18)$$

Using the summation equation for all the nearby elements for F, G and H (equations (19-21)).

$$\bar{F} = \sum\frac{F\Delta x}{\Omega_i} \quad (19)$$

$$\bar{G} = \sum\frac{G\Delta y}{\Omega_i} \quad (20)$$

$$\bar{H} = \sum\frac{H\Delta z}{\Omega_i} \quad (21)$$

Tetrahedral Meshed Shapes

The body shape has to be meshed to find the values by the FVM. The program in this study is developed for only tetrahedral shapes. The advantage of this method is that any shape can be applied in this method. The requirements are only the mesh positions, connectivity and the boundary condition. Therefore the mesh node positions can be import from any software to the program.

Figure 2 shows the example of the pyramids that attached to a single node. All the properties should be solved using the values of all attached nodes. In this study the values of all attached nodes should feed into equation (48-50).

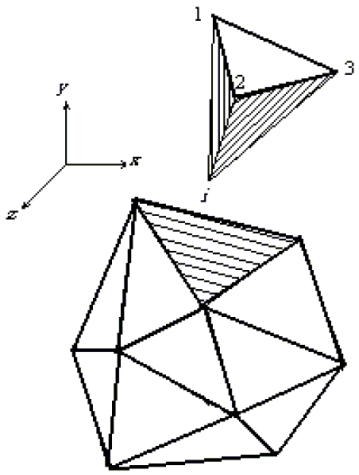

Figure 2: Each node values are calculated with the attached node values, elements and volumes.

Figure 3 shows the projection of the triangle in x, y and z planes. The values for the $\Delta sx, \Delta sy$ and Δsz should be known for the main equations (45-47).

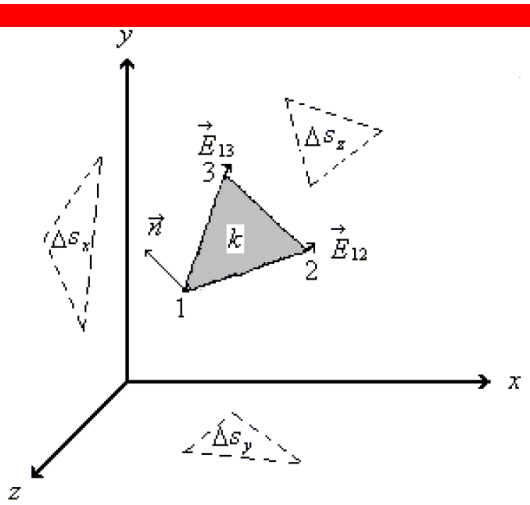

Figure 3: The projection of the triangle, in different planes should obtain for the FVM.

Results of the Program

The program reads the data of the node positions, connectivity, initial and boundary conditions. Then it calculates all the element volumes and surface projections. Then it uses the iteration method to solve the matrix of the equations (45-50) for all nodes. Two model had been applied in the program to find the values of the stress and strain.

EXAMPLE 1

The first model is the simplest model. A simple cube which departs into 8 cube and consists of 27 nodes (Figure 4).

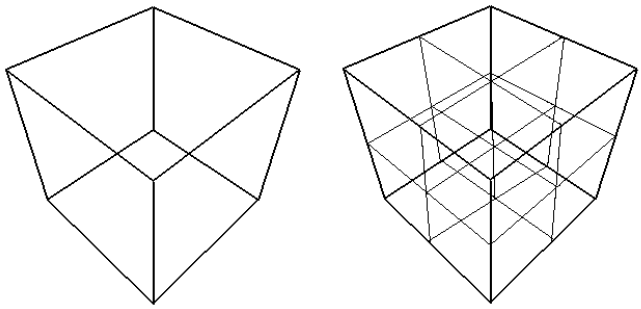

Figure 4: Shape of body in Example 1 which departs to 27 points.

Each cube divides into 5 pyramids, as in Figure 5. Therefore there is 40 pyramids totally, with the volumes of 1/6 and 2/6. The values for all the pyramids attached to each node engaged to the result for the node. In this case, it ranges from 1 to 32 pyramids attached to these 27 nodes.

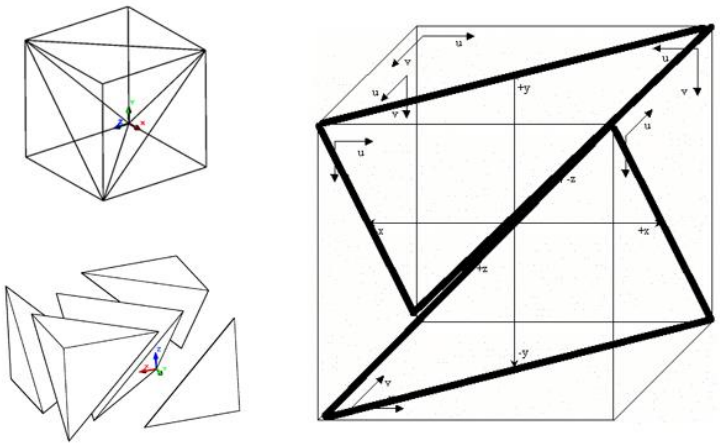

Figure 5: Each cube consists of 5 pyramids, and totally there is 40 pyramids is this example.

The result of strain is obtained as the Figure 6. This result is for strain in x direction for the mid level of the cube. It can be rotated in any view. These results are obtained for different applied horizontal stresses.

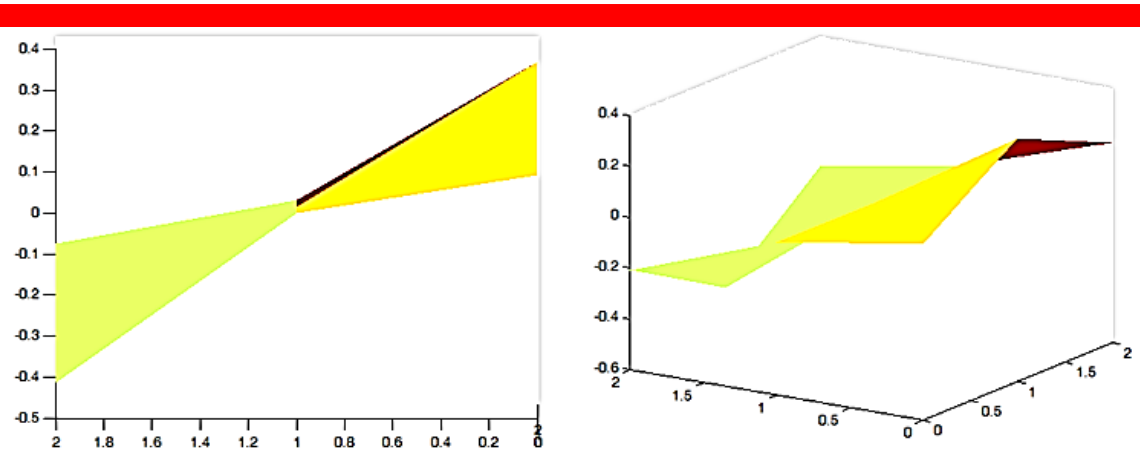

Figure 6: The resulted values of the strain for the mid-level.

If the applied horizontal stresses becomes the same, the graph will be symmetric, as in Figure 7.

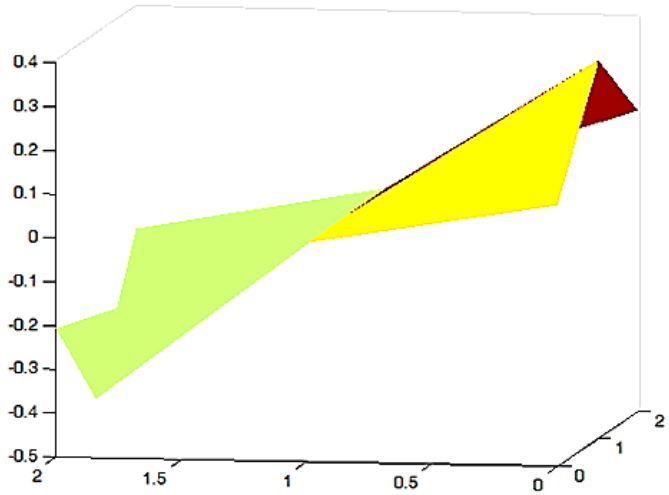

Figure 7: Strain for the mid-level for equal values of horizontal in-situ stresses.

The values of the stress also will find by putting the values of the strains, pressures, and temperatures in the main equation. Figure 8 is the obtained result of stress for the mid level of the cube.

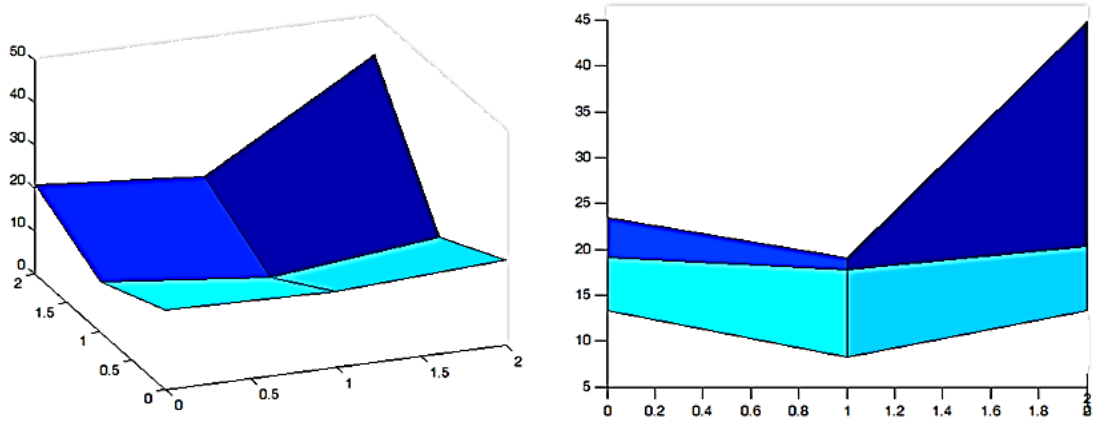

Figure 8: Stress values for the mid-level.

EXAMPLE 2

In order to obtain stress and strain result of the wellbore, the shape of the model has to be sketched (Figure 9).

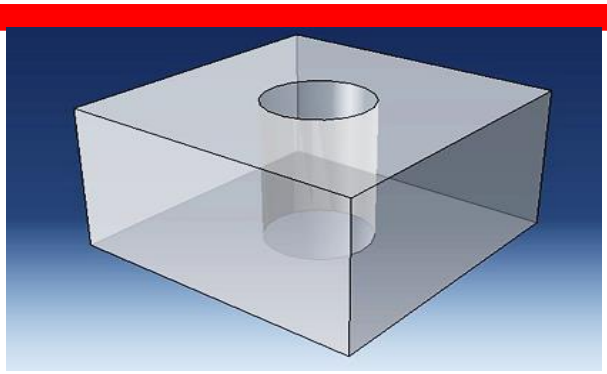

Figure 9: Shape of study in Example 2.

Then it has to be meshed (Figure 10). This meshing can be provided using any mesh generator software, which can feed the nodes and connectivity to the program (Figure 11). The rest will be done by the program.

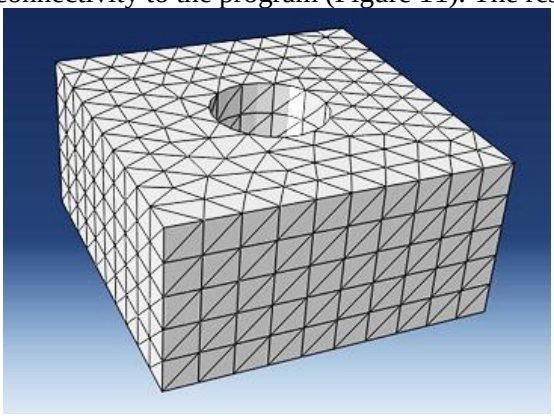

Figure 10: Meshed shape for the FVM.

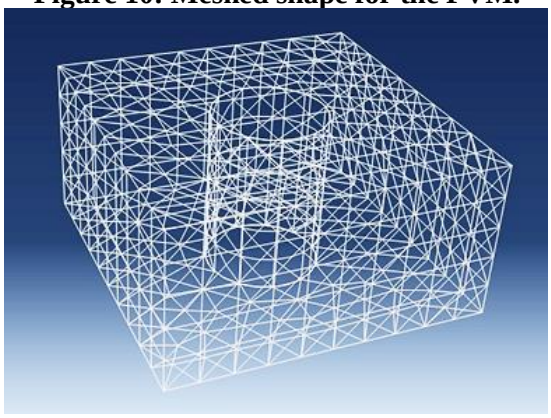

Figure 11: The nodes positions and scheme of connectivity.

The result of stress for this model of wellbore is presented in Figure 12.

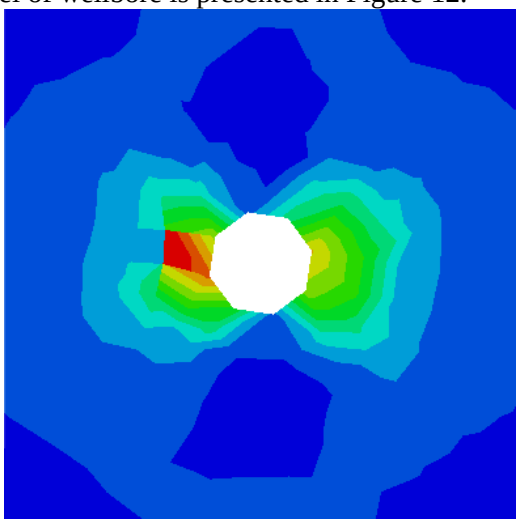

Figure 12: Stress values for the mid-level in Example 2.

CONCLUSIONS

The stress and strain have calculated by the FVM. The values is obtained for two cases of the meshed body; and it can apply on any meshed body. The wellbore shape is meshed and only one scheme of pressure and temperature distribution had applied on the model to see the effects in the stress.

The equal values and different values of the in-situ stresses had applied. In the equal values stress only changes radially but in the different values of the horizontal maximum and minimum stresses the stress changes both in radius and angles.

NOMENCLATURES

I identity tensor (dimensionless)
t time (seconds)
α_T linear thermal expansion
α Biot's constant for a porous media (dimensionless)
β turbulency factor
ε total strain tensor (dimensionless)
σ macroscopic total stress tensor (tension positive) (MPa)
∇A gradient of a vector
r radius (m)
P Pressure (Psi, MPa)
θ angle
i position indicator
n time indicator
λ module of elasticity
G module of rigidity
u, v , w deformation in the direction of x, y and z respectively
F, G, H strain in the direction of x, y and z respectively (same as ε_x, ε_y and ε_z)
Δsx, y, z projection of the triangle in x, y and z planes
k bulk modulus
k_s bulk modulus of the solid phase
k_f bulk modulus of the fluid phase
ζ fluid strain
FVM finite volume method
FDM finite difference method

REFERENCES

[1] Chin L. Y., L. K. Thomas, J. E. Sylte and R. G. Pierson: Iterative Coupled Analysis of Geomechanics and Fluid Flow for Rock Compaction in Reservoir Simulation, *Oil & Gas Science and Technology*, **57**, (2002), Issue no. 5, 485-497.

[2] Du J., R. C. K. Wong: Development of a Coupled Geomechanics-Thermal Reservoir simulator Using Finite Element Method, Canadian International Petroleum Conference, Calgary, Alberta, (2005).

[3] Espinoza, C.E., INTEVEP, S.A.: A New Formulation for Numerical Simulation of Compaction, Sensitivity Studies for Steam Injection, SPE Reservoir Simulation Symposium, San Francisco, California, (1983).

[4] Bataee, M., & Irawan, S. (2014). Review of Geomechanical Application in Reservoir Modeling. Journal of Applied Sciences, 14(10).

[5] M. Bataee, S. Irawan, (2014), "The Effects of Geomechanics on the WAG Injection Model", Offshore Technology Conference-Asia, 25-28 March, Kuala Lumpur, Malaysia

[6] Lewis R. W., C. E. Majorana, B. A. Schrefler.: A coupled finite element model for the consolidation of nonisothermal elastoplastic porous media, *Journal of Transport in Porous Media*, **1**, (1986), Issue no. 2, 155-178.

[7] Lewis R. W., P. J. Roberts, B. A. Schrefler.: Finite element modelling of two-phase heat and fluid flow in deforming porous media, *J. of Transport in Porous Media*, **4**, (1989), Issue no. 4, 319-334.

[8] Lewis R. W., B. A. Schrefler.: The finite element method in the static and dynamic deformation and consolidation of porous media, ISBN: 978-0-471-92809-6, 508 pages, (1998).

[9] Pao W. K. S., R. W. Lewis, I. Masters.: A fully coupled hydro-thermo-poro-mechanical model for black oil reservoir simulation, *International Journal for Numerical and Analytical Methods in Geomechanics*, **25**, (2001), Issue no. 12, 1229–1256.

[10] Yin, S., M.B. Dusseault, and L. Rothenburg: Multiphase poroelastic modeling in semi-space for deformable reservoirs, *Journal of Petroleum Science and Engineering*, **64**, (2009), 45-54.

[11] Yin, S., M.B. Dusseault, and L. Rothenburg: Thermal reservoir modeling in petroleum geomechanics, *International journal for numerical and analytical methods in geomechanics*, **33**, (2009), Issue no. 4, 449-485.

[12] S. Mohseni, M. Bataee., (2011). "Application of Artificial Intelligent Systems in ROP Optimization: a Case Study", SPE Middle East Unconventional Gas Conference and Exhibition, 31 January-2 February, Muscat, Oman.

[13] S. Edalatkhah, et al., (2010), "Comparison between Bit Optimization Using Artificial Neural Network and Other Methods Base on Log Analysis Applied in Shadegan Oil Field", International Oil and Gas Conference and Exhibition in China, 8-10 June, Beijing, China

[14] M. Bataee, S. Irawan, (2014), "Artificial Neural Network Model for Prediction of Drilling Rate of Penetration and Optimization of Parameters", Journal of the Japan Petroleum Institute 57(2), 65-70, 2014-03.

[15] Ali Ghalambor, et.al., (2010), "Neural Networks in BHCP Prediction Performed Much Better Than Mechanistic Models", International Oil and Gas Conference and Exhibition in China, 8-10 June, Beijing, China.

[16] M. Bataee., M. Kamyab., (2010), "Investigation of Various ROP Models and Optimization of Drilling Parameters for PDC and Roller-cone Bits in Shadegan Oil Field",International Oil and Gas Conference and Exhibition in China, 8-10 June, Beijing, China.

[17] M.R. Zare, et al., (2012), "Production Optimization Using Different Scenarios of Gas Lift and ESP Installation".,World Applied Sciences Journal, 17 (4), 524-531.